Key Engineering Materials Vols. 340-341 (2007) pp. 1115-1120
online at http://www.scientific.net

Seismic Damage Characteristics of RC Shear Wall with Diagonal Profile Steel Braces by Experiment

Shi-Yun Xiao[1,a], Hong-Nan Li[1,b], Yan-Gang Zhao[2,c] and Jing-Wei Zhang [1,d]

[1)] The State Key Laboratory of Coastal and Offshore Engineering, Dalian University of Technology, Dalian 116024, China

[2)] Department of Civil and Arthitectural Engineering, Nagoya Institute of Technology Nagoya, Japan

[a)] shyxiao@dlut.edu.cn, [b)] hnli@dlut.edu.cn, [c)] zhao@ nitech.ac.jp, [d)] 2002jwzhang@163.com

Key words: shear wall; profile steel; bearing capacity; ductility; hysteretic loop

Abstract. This paper focuses on an experimental investigation and theoretical analysis of different types of RC shear wall with the profile steel braces in two side columns and diagonal profile steel braces of walls subjected to applied repeated cyclic loads. Fifteen RC shear walls with different shear span ratio are tested and their aseismic charactertics are studied. The effect of profile steel bracings on failure property, bearing capacity, ductility and hysteretical characteristic of shear wall is investigated based on experimental results. It is shown that adding the profile steel braces on the boundary column and inner of walls can obviously enhance the ultimate strength of specimens and improve their aseismic characteristics. Finally, the mechanical model of the shear wall is presented and the formulae for calculating the load-carrying capacity are developed. Numerical analyses indicate that the theoretical results agree well with those from experiments.

Introduction

Recently, more and more skyscrapers are designed and built one after the other. These high-rise buildings require more excellent load-bearing capacity of RC shear wall. In normal case, these requirements may be satisfied by increasing the reinforcement ratio and section size of the walls. Yet at the same time, the cost of structures increases greatly and the space of buildings is compressed so that the structural deadweight increases sharply. In order to satisfy the demands of load-bearing capacity and aseismic requirements, many new types of RC shear walls are developed.

M.R. Maheri et al.[1] made the use of steel braces in concrete-framed structures to determine the effectiveness of different diagonal bracing arrangements to increase the in-plane shear strength of the concrete frame. L. Galano et al.[2] investigated the seismic response of the coupled system of masonry structures by joining shear walls with the steel X-brace in the time domain. K.A. Zalka[3] studied the characteristic deformations and stiffnesses of multistory frameworks with the cross-braces. They presented the formulae for the shear stiffness of cross-braces of different geometrical arrangements.

In order to improve the seismic behavior of low - rise reinforced concrete (RC) shear walls, H. Liu et al.[4] tested shear walls of the low– rise steel-encased reinforced concrete (SRC) with steel skeletons embedded in. Based the result of the experiment, Z.H. Wang et al.[5] introduced the application of the low-rise SRC shear walls to multistory masonry buildings as a reference in the anti-seismic design of multistory masonry buildings with large space in its bottom. W.L. Cao et al.[6] proposed a new type of RC shear wall with concealed braces. They carried out four 1:3 scale medium-height shear wall specimens that are composed of three pieces of shear walls with

X-shaped concealed steel-bar braces, in which the load-carrying capacity, stiffness, ductility, hysteretic behavior and energy dissipation of these shear walls were studied. They also investigated the effect of reinforcement ratio[7] and inclination of concealed braces[8] on aseismic property of shear walls. Finally, they proposed a mechanical model of the shear wall and formulae for calculating load-carrying capacity developed[9].

In order to develop the new shear wall system with better property, this paper focuses on an experimental investigation and theoretical analysis of different types of RC shear wall with diagonal steel braces subjected to applied repeated cyclic loads. Fifteen RC shear walls are tested and their aseismic characteristics are studied. Finally, the mechanical model of the shear wall is presented and the formulae for calculating the load-carrying capacity are developed.

Experiment

Descriptions of wall samples. Fifteen RC shear wall samples are built and tested in the project. They have the same cross section size. All pedestals and loading beams of shear walls have same configuration. To meet the needs of flexural and ductile features, the walls are designed with boundary columns at each side of walls. Fifteen walls are divided into three groups according to their shear span ratios: 1.0:1, 1.5:1 and 2.0:1, respectively. Each group of samples includes three types of walls: one piece of normal RC shear wall, one piece of RC shear wall with profiled steel braces only in the side columns and three pieces of RC shear wall with profiled steel braces in the side columns and oblique profiled steel braces in the wall. The parameters of samples are listed in Table 1. Figure 1 gives the size and shape of RC shear walls named as the sw1-2, sw1-3 and sw1-4.

Table 1 Parameters of wall samples

Specimen	Steel ratio in column	Transverse reinforcement ratio	Shear span ratio
sw1-1		0.25%	1
sw1-2	1.43%	0.25%	1
sw1-3	1.43%	0.25%	1
sw1-4	1.43%	0.25%	1
sw1-8	1.43%	0.25%	1
sw2-1		0.28%	1.5
sw2-2	1.43%	0.28%	1.5
sw2-3	1.43%	0.28%	1.5
sw2-4	1.43%	0.28%	1.5
sw2-8	1.43%	0.28%	1.5
sw3-1		0.29%	2
sw3-2	1.43%	0.29%	2
sw3-3	1.43%	0.29%	2
sw3-4	1.43%	0.29%	2
sw3-8	1.43%	0.29%	2

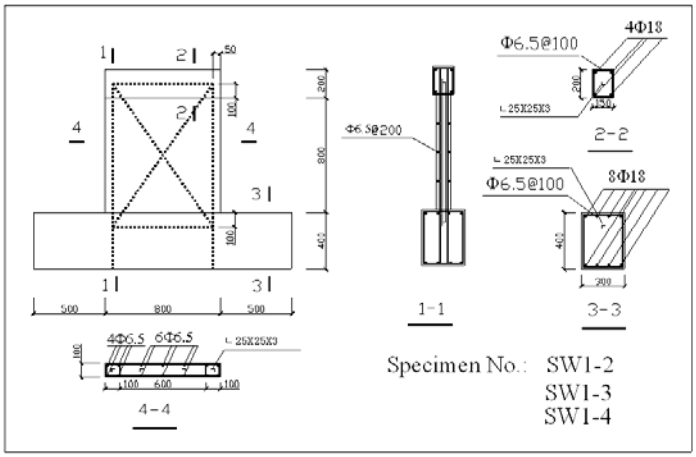

Fig.1 Sketch of size and shape of shear walls

Experimental setup. The shear wall samples were loaded in the steel frame shown in Figure 2. The horizontal load was applied by two 1000*KN* hydraulic jacks and was controlled by the loading transducers connected to the jacks. Two ball joints were installed for the stabilization of horizontal load. The axial compressive forces on the wall were provided by a 1000KN hydraulic jack connected to the loading transducer and ball joint. A steel channel was placed on the top of wall and two steel plates on the sides of loading beam to facilitate a loading transfer from the load actuators to the wall and to confine the concrete to prevent a local compression failure. The displacement transducer was applied to the midpoint of top of specimen. The

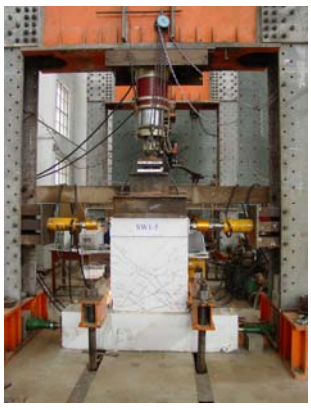

Fig.2 Test setup

horizontal and vertical loadings and the top displacement of the sample were collected with the high speed data acquisition system, and these data were analyzed and the curves of the horizontal loading versus the top displacement of the wall were figured with the MTLab software.

Experimental results and analysis

Cracking process and failure mode. For the specimens that shear span ratio is 1.0, the failure behavior of specimen sw1-1 showed the obvious frangibility and belonged to base shear failure. The crack pattern is shown in Fig.3(a). The cracking pattern of sw1-8 was just like the specimen sw1-1. The behavior performed obvious frangibility and belonged to shear failure and the crack pattern is illustrated in Fig.3(b). The behaviors of sw1-2, sw1-3 and sw1-4, are similar to those of sw1-8 before failure. The destroy characteristic of specimen didn't show obvious frangibility and belonged to shear-bending failure mode. The crack pattern of the sw1-2 is shown in Fig.3(c).

For the specimens that shear span ratio is 1.5, the cracking process and failure mode of specimen sw2-1 were similar with the specimen sw1-1. The failure behavior belonged to the base shear failure and showed the obvious frangibility. Its crack pattern is shown in Fig.3(d). The behavior of the wall sw2-8 performed obvious frangibility and belonged to shear failure. Its crack pattern is illustrated in Fig.3(e). The behaviors of specimens, sw2-2, sw2-3 and sw2-4, are similar to those of sw2-8 before failure. These destroy characteristic didn't show obvious frangibility and belonged to shear-bending failure mode. The crack pattern of sw2-3 is shown in Fig.3(f).

For the specimens that shear span ratio is 2.0, the behavior of specimen sw3-1 showed the obvious ductility and belonged to bending failure mode. The crack pattern of the sw3-1 is shown in Fig.3(g).The behaviors of specimen sw3-8 were similar to those of sw3-1, and the failure behavior showed the obvious ductility and belonged to bending failure mode. The crack pattern is illustrated in Fig.3(h). The behaviors of specimens, sw3-2, sw3-3 and sw3-4, were absolutely similar to those of the sw3-8. And the behavior of specimen showed more obvious ductility and also belonged to bending failure mode. The crack pattern of the sw3-2 is shown in Fig.3(i).

(a) sw1-1 (b) sw1-8 (c) sw1-2 (d) sw2-1 (e) sw2-8

f) sw2-3 (g) sw3-1 (h) sw3-8 (i) sw3-2

Fig.3 Failure behavior of specimens

Hysteretic curves of shear wall. The hysteretic curve of shear wall can reflect the dissipating energy capacity. Fig.4 depicts the hysteretic curves of shear walls at the shear-span ratio 1.0, 1.5 and 2.0, respectively. Compared with the normal RC shear wall, the hysteretic loops of shear walls, which boundary columns have profile steel bracings, are plump and more increasing the diagonal profile steel at the wall, the hysteretic loops become more plump. Hence, it can be concluded that increasing the profile steel in the boundary columns and wall can considerably improve the ductility and carrying capacity of a shear wall.

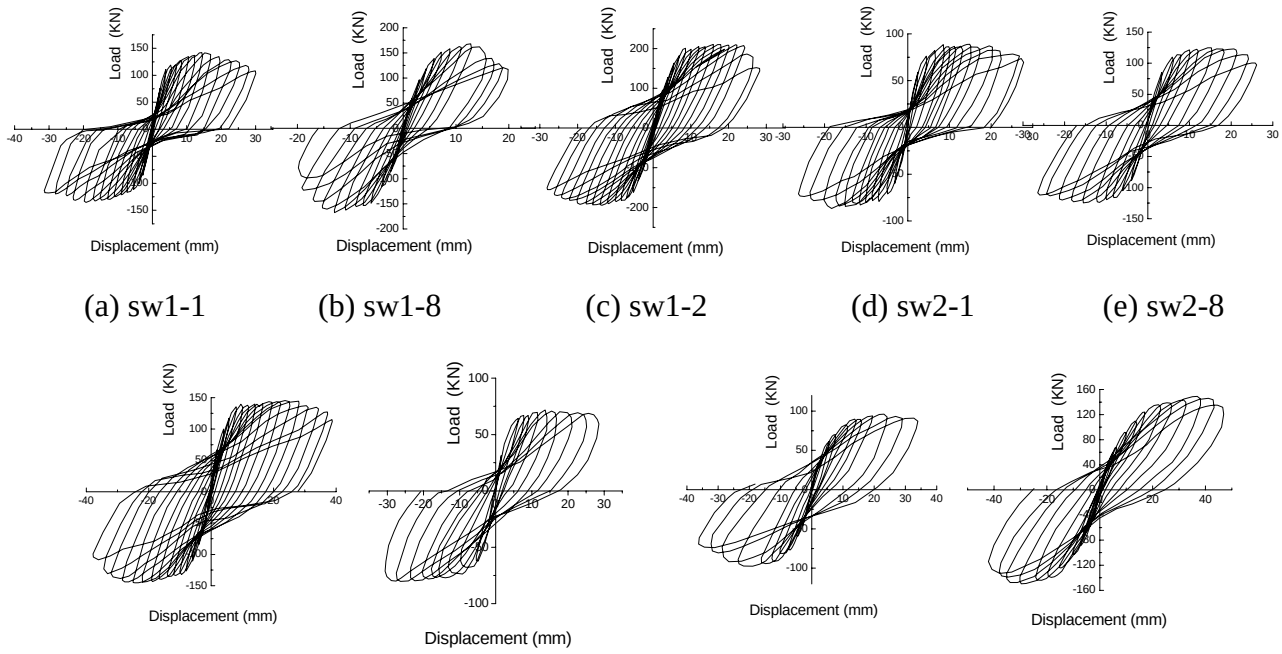

(a) sw1-1 (b) sw1-8 (c) sw1-2 (d) sw2-1 (e) sw2-8

f) sw2-3 (g) sw3-1 (h) sw3-8 (i) sw3-2

Fig.4 Hysteretic curves of specimens

Carrying capacity of shear wall. Table 2 lists the cracking strengths, P_{c}, and the ultimate bearings, P_{u}, of fifteen shear walls, where P_{c} and P_{u} are the average of strengths in two horizontal directions, respectively. The results show that the cracking strengths of the same group walls vary little because the profile steel bracings of walls have almost no effect on the initial stiffness of walls within the elastic range. However, the ultimate strengths of walls are different largely. The profile steel braces of walls played a dominant role after cracking of walls so that the ultimate bearings increase sharply. Compared with the normal RC shear wall, the ultimate bearings of shear walls with the profile steel strengths only in two side columns increase with 22.5% (λ =1.0), 46.1% (λ =1.5) and 23.8% (λ =2.0), respectively, and the ultimate bearings of shear walls with both the profile steel strengths in two side columns and diagonal profile steel braces in walls increase with 44.2% (λ =1.0), 75.2% (λ =1.5) and 37.5% (λ =2.0), respectively.

Table 2 Cracking and ultimate strength

Specimen No.	P_c (KN)	P_u (KN)	P_u/P_c
sw1-1	80	138	1.73
sw1-2	97	201	2.07
sw1-3	84	192	2.29
sw1-4	82	204	2.49
sw1-8	91	169	1.86
sw2-1	60	83.5	1.39
sw2-2	64.5	147	2.28
sw2-3	64.5	143	2.22
sw2-4	67	149	2.22
sw2-8	62.5	122	1.95
sw3-1	56	80	1.43
sw3-2	69	146	2.12
sw3-3	60	111	1.85
sw3-4	60	109	1.82
sw3-8	59	99	1.68

Ductility of shear walls. Table 3 lists the cracking displacements, Δ_c, and the ultimate displacements, Δ_u, of fifteen shear walls, where Δ_c and Δ_u are the average of displacements in two

horizontal directions, respectively. The results show that the cracking displacements of the same group walls vary little because the profile steel bracings of walls have almost no effect on the initial stiffness of walls within the elastic range. However, the ultimate displacements of shear walls are different considerably. Dissimilar to the ultimate strengths of shear walls, the ultimate displacements of shear walls with the profile steel strengths only in two side columns vary little compared with the normal RC shear walls. It is because the profile steel braces in side columns have little effect on the shear stiffness of shear walls. Similar to the ultimate strengths of shear walls, the ultimate displacements of walls with both the profile steel strengths in two side columns and diagonal profile steel braces in walls increase sharply because the diagonal profile steel braces of walls played a dominant role close to failure of shear walls. Compared with the normal RC shear wall, the ultimate displacements of shear walls with both the profile steel strengths in two side columns and diagonal profile steel braces in walls increase with 26.7% (λ =1.0), 51.0% (λ =1.5) and 46.7% (λ =2.0), respectively.

Table 3 Cracking and ultimate displacement

Specimen No.	Δ_c (mm)	Δ_u (mm)
sw1-1	2.5	15
sw1-2	2.6	20
sw1-3	2.2	17
sw1-4	2.2	20
sw1-8	2.0	14
sw2-1	1.7	16
sw2-2	2.7	22.5
sw2-3	2.0	25
sw2-4	2.4	25
sw2-8	1.8	16.5
sw3-1	4.0	20
sw3-2	4.5	32
sw3-3	4.4	30
sw3-4	4.6	26
sw3-8	5.0	21.2

Formulation of carrying capacity of shear wall

Calculation model of shear walls. According to the failure mode of specimens and the strain of reinforcements and profile steels, it can be seen that the bending or shear-bending failure modes take place in middle and high shear walls and the moment action at the base section is a important factor on the carrying capacity of shear walls. According to experiment results, the calculation model of RC shear wall with both the profile steel strengths in two side columns and diagonal profile steel braces is assumed and illustrated in Fig.5.

Calculation formula of carrying capacity. According to the analysis of the above section, the calculation formulae of carrying capacity are derived as follow:

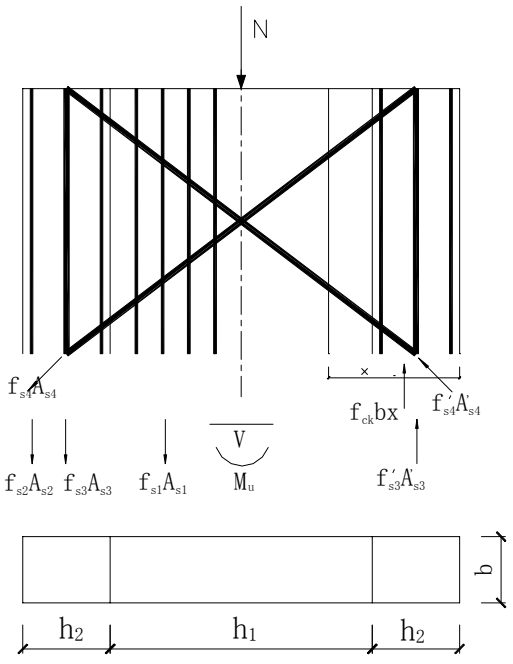

Fig.5 Calculation model

The simplified model of equivalent rectangular stress block is as follows

$$f_{y1}A_{s1} + f_{y2}A_{s2} + f_{y3}A_{s3} + f_{y4}A_{s4}\sin\alpha + N - f'_{y2}A'_{s2} - \gamma\cdot(f'_{y3}A'_{s3} + f'_{y4}A'_{s4}\sin\alpha) - f_{ck}bx = 0 \qquad (1)$$

The ultimate moment acting on wall section

$$M_u = f_{y1}A_{s1}(\frac{3h_1}{4} + h_2 - \frac{x}{2}) + f_{y2}A_{s2}(h_1 + \frac{3h_2}{2} - \frac{x}{2}) - f'_{y2}A'_{s2}(\frac{h_2}{2} - \frac{x}{2}) + f_{y3}A_{s3}(h_1 + \frac{3h_2}{2} - \frac{x}{2})$$
$$-\gamma\cdot f'_{y3}A'_{s3}(\frac{h_2}{2} - \frac{x}{2}) + f_{y4}A_{s4}\sin\alpha(h_1 + h_2 - \frac{x}{2}) - \gamma\cdot f'_{y4}A'_{s4}\sin\alpha(h_2 - \frac{x}{2}) + N(\frac{h_1}{2} + h_2 - \frac{x}{2}) \qquad (2)$$

The horizontal loading acting on the top of shear wall

$$P_u = M_u / H \tag{3}$$

Where, γ is the interaction-influencing coefficient of oblique profile steel and vertical profile steel, which is related to the span ratio λ of the shear walls. According to the analytical results of experimental data, it can be drawn as follows: when λ=1.0, γ=0.8; when λ=1.5, γ=0.6; when λ=2.0, γ=0.4.

Comparisons of carrying capacity of calculated results with experimental results. According to above formulae, the numerical results of carrying capacity of 12 specimens are obtained and compared with the experimental results, as listed in Table 4. Except the shear wall sw3-2, the calculated results of the other shear walls correspond with the experimental results and the errors are under 15%. Compared with the shear walls sw3-3 and sw3-4, the carrying capacity of sw3-2 is higher and that can be explained with the dispersal of concrete.

Table 4 Comparisons of carrying capacity

Specimen No.	Calculation Result (*KN*)	Experimental Result (*KN*)	Error (%)
sw1-2	202.9	201	-0.94
sw1-3	202.9	192	-5.37
sw1-4	202.9	204	0.54
sw1-8	164.9	169	2.49
sw2-2	143.1	147	2.73
sw2-3	143.1	143	-0.07
sw2-4	143.1	149	4.12
sw2-8	112.9	122	8.06
sw3-2	112.0	146	30.36
sw3-3	112.0	111	-0.89
sw3-4	112.0	109	-2.68
sw3-8	86.8	99	14.06

References

[1] M.R. Maheri and A. Sahebi: Use of steel bracing in reinforced concrete frames. Engineering Structures Vol. 19 (1997), p. 1018

[2] L. Galano and V. Gusella: Reinforcement of masonry walls subjected to seismic loading using steel X-bracing. Journal of Structural Engineering Vol. 124 (1998), p. 886

[3] K.A. Zalka: Full-height buckling of frameworks with cross-bracing. Proceedings of the Institution of Civil Engineers, Structures and Buildings Vol. 134 (1999), p. 181

[4] H. Liu, Z.J. Lan and T.H. Pang: Test and analysis on seismic behavior of low-rise steel-encased reinforcement concrete shear walls. Industrial Construction Vol. 27 (1997), p. 32

[5] Z.H. Wang and Z.J. Lan: The application of low-rise steel-encased RC shear wall in multistory masonry building with large space in its bottom. Journal of Hiangnan Collloge Vol. 13 (1998), p. 46

[6] W.L. Cao, S.D. Xue and J.W. Zhang: Seismic performance of RC shear walls with concealed bracing. Advances in Structural Engineering Vol. 6 (2003), p. 1

[7] C.Y. Liu, W.L. Cao and J.W. Zhang: Influence of reinforcement ratio of concealed bracing on aseismic property of the RC shear wall. World Information of Earthquake Engineering Vol. 16 (2000), p. 73

[8] W.L. Cao, C.Y. Liu and J.W. Zhang: Influence of Inclination of concealed bracing on aseismic property of the RC shear wall. World Information of Earthquake Engineering Vol. 16 (2000), p. 68

[9] W.L. Cao, M.J. Zhou and C.S. Hao: Experimental and calculation analysis on aseismic consumed energy behavior of shear wall with concealed bracings. Journal of Hebai University of Technology Vol. 29 (2000), p. 57